Journal of Molecular Structure 1142 (2017) 217–225

Contents lists available at ScienceDirect

Journal of Molecular Structure

journal homepage: http://www.elsevier.com/locate/molstruc

Crystal structure, Hirshfeld surface, physicochemical, thermal and DFT studies of (N^1E, N^2E)-N^1,N^2-bis((5-bromothiophen-2-yl)methylene) ethane-1,2-diamine N_2S_2 ligand and its [$CuBr(N_2S_2)$]Br complex

Ismail Warad [a, *], Yasmin Al-Demeri [a], Mohammed Al-Nuri [a], Said Shahwan [a], Muneer Abdoh [b], Shivalingegowda Naveen [c], Neartur Krishnappagowda Lokanath [d], Mohammad S. Mubarak [e], Taibi Ben Hadda [f], Yahia N. Mabkhot [g]

[a] Department of Chemistry, Science College, An-Najah National University, P.O. Box 7, Nablus, Palestine
[b] Department of Physics, Science College, An-Najah National University, P.O. Box 7, Nablus, Palestine
[c] Institution of Excellence, Vijnana Bhavana, University of Mysore, Manasagangotri, Mysuru, 570 006, India
[d] Department of Studies in Physics, University of Mysore, Manasagangotri, Mysuru, 570 006, India
[e] Department of Chemistry, The University of Jordan, Amman, 11942, Jordan
[f] Laboratoire Chimie Matériaux, FSO, Université Mohammed 1ER, Oujda, 60000, Morocco
[g] Department of Chemistry, College of Science, King Saud University, P.O. Box 2455, Riyadh, 1451, Saudi Arabia

ARTICLE INFO

Article history:
Received 20 December 2016
Received in revised form
15 April 2017
Accepted 17 April 2017
Available online 21 April 2017

Keywords:
Copper(II) complexes
Tetradentate
N_2S_2 Schiff base
XRD
DFT

ABSTRACT

A new tetradentate N_2S_2 Schiff base ligand derived from 5-bromothiophene-2-carbaldehyde and its [$CuBr(N_2S_2)$]Br complex were synthesized in good yield. FT-IR was investigated to monitor the condensation reaction during the ligand synthesis process. The ligand, N_2S_2, and its complex, [$CuBr(N_2S_2)$]Br, complex have been characterized with the aid of several spectroscopic techniques such as UV–vis., MS, FT-IR, EA, EDS, NMR (for N_2S_2), as well as by thermal (TG/DTG) analysis. In addition, cyclic voltammetry has been employed to examine the redox behavior of [$CuBr(N_2S_2)$]Br complex in N,N'-dimethylformamide (DMF) containing 0.10 M tetra-*n*-butylammonium perchlorate (TBAP). The anti-conformation *EE* isomer of the ligand (N_2S_2) was confirmed by means of X-ray crystallography; ligand crystallizes in to the monoclinic $P2_1/c$ space group. N_2S_2 ligand was subjected to DFT-theoretical calculations and results are consistent with the experimental chemical analysis.

1. Introduction

Schiff bases, a class of organic compounds with a variety of interesting properties, continue to attract the attention of chemists owing partly to the significant physical and chemical properties of their metal complexes. In addition they constitute a special type of unsaturated poly-atoms organic ligands [1–5]. Many types of such Schiff bases have been synthesized and their biological, physical, and chemical properties investigated [2–6]. Moreover, Schiff base as N-ligands possess broad scope of industrial applications such as catalysts [6–8], metal ions sensors [9], and photochromic [10]. Several Schiff bases display remarkable biological activity such as antitumor [11], antiviral [12], antifungal [13], antimicrobial [14], anticancer [15] and antibacterial [16,17].

In coordination chemistry, N- and S-containing Schiff-base ligands play a critical role in the construction of new metal ions complexes [17–20]. Since such ligands hold both soft sulfur and hard nitrogen atoms as donors, they can coordinate with a broad range of metal ions, which lead to forming several types of complexes with their interesting biological and physicochemical properties [16–20]. Schiff bases and their starting material amines behave as polydentate chelating ligands, their complexes are becoming rather important for their various structures and extensive applications [21–23]. One of the prominent multidentate N_2S_2 Schiff-base ligands, especially the one which contains thiophene derivatives functional groups that attracted the attention of researchers, mainly due to their ability to coordinate metals *via* several sites, in addition to their pharmaceutical and medicinal chemistry importance [24–26].

Furthermore, due to redox behavior of copper (II) complexes

* Corresponding author.
E-mail address: warad@najah.edu (I. Warad).

http://dx.doi.org/10.1016/j.molstruc.2017.04.064
0022-2860/

and their interaction capability with DNA, causing cell apoptosis and DNA damage, these complexes could serve as substitutes to platinum-complexes drugs specially cis-platin [23–26]. The electronic properties and special coordination structure of such complexes reveal a non-covalent interaction with the DNA intercalation or electrostatic interaction modes [24–30]. In view of the broad interest in Schiff base–metal complexes, and owing to the physical and biological importance of these species, we describe herein the synthesis, characterization, XRD and DFT theoretical studies of the tetradentate N_2S_2 Schiff base ligand and its mono-cationic $[CuBr(N_2S_2)]Br$ complex.

Table 1
N_2S_2 Crystal data and structure refinement details.

CCDC Number	CCDC	
Empirical formula	$C_{12}H_{10}Br_2N_2S_2$	
Formula weight	406.16	
Temperature	293(2) K	
Wavelength	1.54178 Å	
Reflns. for cell determination	2267	
θ range for above	4.05°–64.48°	
Crystal system	Monoclinic	
Space group	$P21/c$	
Cell dimensions		
$a = 10.914(3)$ Å	$b = 4.4864(18)$ Å	$c = 30.692(9)$ Å
$\alpha = 90.00°$	$\beta = 91.264(13)°$	$\gamma = 90.00°$
Volume	1502.4(9) Å^3	
Z	4	
Density (calculated)	1.796 Mgm^{-3}	
Absorption coefficient	9.310 mm^{-1}	
F_{000}	792	
Crystal size	0.3 × 0.27 × 0.25 mm	
θ range for data collection	4.05°–64.48°	
Index ranges	$-12 \le h \le 12$	
	$-2 \le k \le 5$	
	$-34 \le l \le 34$	
Reflections collected	4662	
Independent reflections	2267 [$R_{int} = 0.0214$]	
Absorption correction	multi-scan	
Refinement method	Full matrix least-squares on F^2	
Data/restraints/parameters	2267/0/163	
Goodness-of-fit on F^2	1.149	
Final [$I > 2\sigma(I)$]	$R1 = 0.0548$, $wR2 = 0.1517$	
R indices (all data)	$R1 = 0.0679$, $wR2 = 0.1739$	
Largest diff. peak and hole	0.906 and −0.920 e Å^{-3}	

2. Experimental

2.1. Material and instrumentation

Chemicals employed throughout this investigation were purchased from Sigma and used as received without purification. Purity of products was checked with TLC. Elemental analysis was carried out on an Elementar-Vario EL analyzer; results agreed with the calculated percentages to within the experimental error (±0.4%). IR spectra were recorded on a Perkin-Elmer Spectrum 1000 FT-IR Spectrometer as KBr pellets, whereas UV–Vis spectra were obtained with a TU-1901-double-beam UV–visible spectrophotometer. NMR spectra were acquired on Bruker DRX 500 with $CDCl_3$ as solvent and TMS as the internal standard; chemical shifts are expressed in ppm. Cyclic voltammograms on a platinum electrode were recorded with the aid of a three-electrode cell Voltalab 80 potential-state. EI-MS data was obtained on a Finnigan 711A mass spectrometer. Thermogravimetric analysis and differential thermal analysis (TG/DTG) for both the ligand and its complex were carried out with a Perkin–Elmer instrument; measurements were done at a heating rate of 10 °C/min over the temperature range of 0–1000 °C.

2.2. Synthesis of N_2S_2 ligand

The title compound was prepared according to the following procedure: 5-bromothiophene-2-carbaldehyde (0.02 mol) was added to ethylenediamine (0.01 mol). When the temperature and viscosity of mixture increased, 20 mL of dichloromethane was added to the mixture to achieve complete solubility. The reaction was stirred for 60 min at room temperature. Yellow colored single crystals were obtained after slow evaporation of the dichloromethane solvent. Yield 90%. IR (KBr, cm^{-1}) $\nu_{max} = 1629$ (C=N), 2890 (C-$H_{aliphatic}$), 3010 (C-$H_{thiophene}$), UV–Vis in EtOH: 295 nm (sharp) and 265 nm shoulder. ^{1}H NMR (500 MHz, $CDCl_3$): δ (ppm): 3.86 (br, 4H, -CH=NCH_2CH_2N=CH-), 6.99 (2H, $^3J_{AB} = 4.75$ Hz, thiophene), 7.01 (2H, $^3J_{AB} = 4.85$ Hz, thiophene), 8.20 (2H, −HC=N)·^{13}C NMR: δ (ppm): 60.65 (2C, -CH=NCH_2CH_2N=CH-), 116.95, 130.34, 130.55, 143.99 (8C, thiophene), 155.21 (2C, −HC=N-). [M^+] = 403.8 m/z. Anal. Calcd. for $C_{12}H_{10}Br_2N_2S_2$: C, 35.49; H, 2.48; N, 6.90; found: C, 35.18; H, 2.29; N, 6.78%.

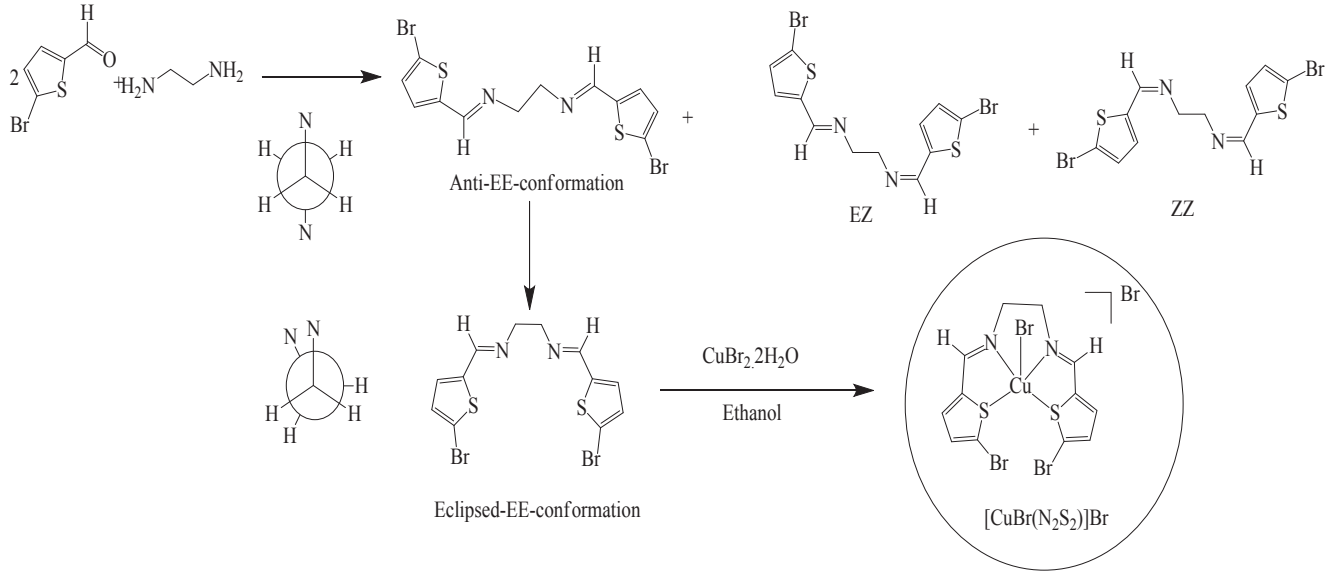

Scheme 1. Synthesis of the N_2S_2 and its desired monocationic $[CuBr(N_2S_2)]Br$ complex.

2.3. Synthesis of [CuBr(N_2S_2)]Br complex

A solution of N_2S_2 (0.20 mmol) dissolved in 8 mL of EtOH was added dropwise to (0.20 mmol) of $CuBr_2 \cdot 2H_2O$ dissolved in 10 mL of EtOH. The temperature of the reaction increased and the color changed (from brown to blue upon mixing of the two reagents) indicated the occurrence of the complexation reaction spontaneously. When the mixture was concentrated by removing some of the solvent under reduced pressure, most of the blue Cu(II) complex precipitated, filtered, and washed well with cold EtOH. Yield 90%, m.p. = 270 °C. MS *m/z* 545.71 [M^{+1}-Br] calc. MS = 547.60. Anal. Calcd for $C_{12}H_{10}Br_4CuN_2S_2$: C, 22.90; H, 1.60; N, 4.45; found: C, 22.76; H, 1.45; N, 4.32%. Conductivity in water: 108 (μS/cm). IR (KBr, νcm^{-1}): 3380 (ν_{H2O}), 2970 ($\nu_{C\text{-}Hthiophene}$), 2860 ($\nu_{C\text{-}H\ aliphatic}$), 1608 ($\nu_{C=N}$), 510, 500 ($\nu_{Cu\text{-}N}$). UV–Vis in water: 275 ($\varepsilon = 1.2 \times 10^4$ $M^{-1}L^{-1}$) and 615 nm ($\varepsilon = 6.4 \times 10^2$ $M^{-1}L^{-1}$).

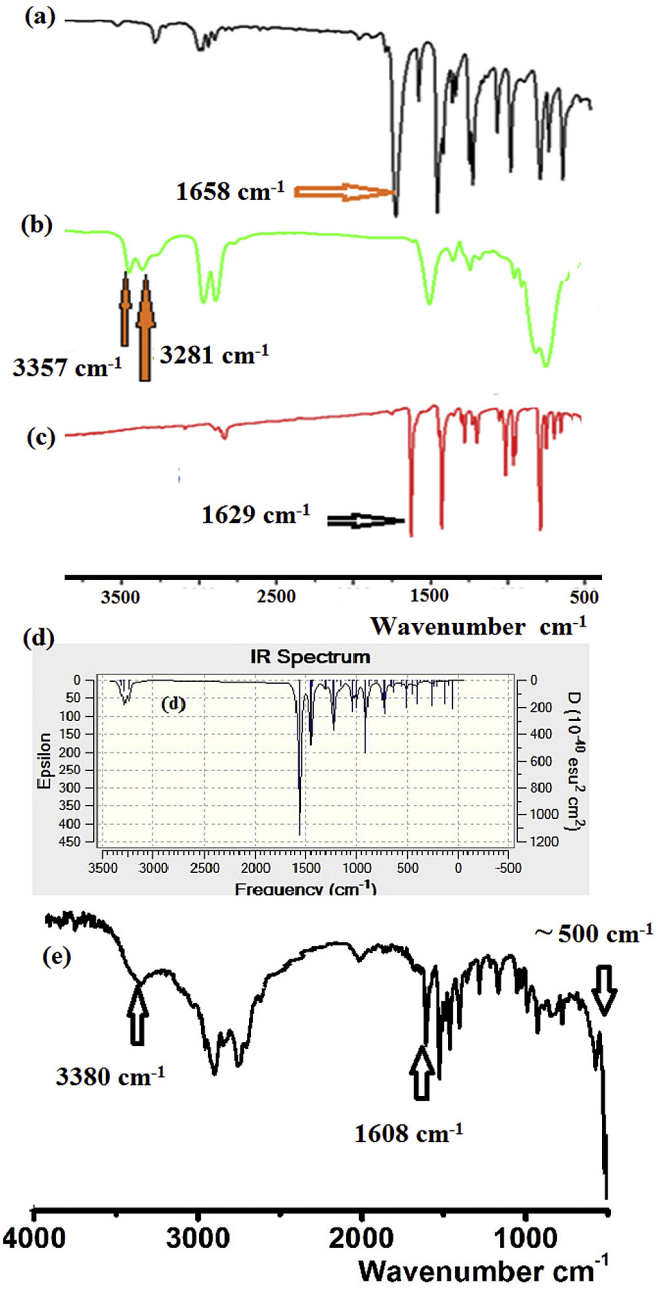

Fig. 1. IR spectra of: (a) 5-bromothiophene-2-carbaldehyde, (b) ethylenediamine, (c) N_2S_2 ligand, (d) DFT/B3LYP 6–311++G (d,p) theoretical calculation of N_2S_2 ligand, and (e) [CuBr(N_2S_2)]Br complex.

2.4. X-ray crystallography

X-ray intensity data were collected at a temperature of 296 K on a Bruker Proteum 2 CCD diffractometer equipped with an X-ray generator operating at 45 kV and 10 mA, using Cu Ka radiation of wavelength 1.54178 Å. Details of the crystal structure and data refinement are given in Table 1. Cell refinement and data reduction were accomplished with the aid of a SAINT PLUS [31], whereas the structure was solved by direct methods and refined by full-matrix least squares method on F2 using SHELXS and SHELXL programs [32]. All the non-hydrogen atoms were revealed in the first difference Fourier map itself. All hydrogen atoms were positioned geometrically and refined using a riding model. Geometrical calculations were carried out using the program PLATON [33].

2.5. Computational analysis

The structure of the desired ligand, as solved by X-ray diffraction, was optimized at DFT/B3LYP [34] using the GAUSSIAN09 [35]. The basis set 6–311++G (d,p) was employed in all theoretical measurements [36]. CRYSTAL EXPLORER 3.1 program was used to perform the Hirshfeld surfaces theoretical analysis of N_2S_2 [37].

3. Results and discussion

3.1. Synthesis

Condensation of 5-bromothiophene-2-carbaldehyde with ethylenediamine in a 2:1 M ratio afforded the tetra-dentate Schiff base (N^1E, N^2E)-N^1,N^2-*bis*((5-bromothiophen-2-yl)methylene)ethane-1,2-diamine [N_2S_2] ligand in a very good yield, as shown in Scheme 1. The EE isomer was found to be favored over any other isomers such EZ or ZZ isomers. Moreover, the EE anti-conformation was sterically favored over EE-eclipsed-conformation isomer. The stable EE anti-conformation was isolated and its structure confirmed by X-ray single crystal diffraction. The desired ligand was found to be soluble in common organic solvents. DFT theoretical calculations of free ligand was performed using Gaussian 09 program.

Treatment of N_2S_2 ligand with equivalent amount of $CuBr_2 \cdot 2H_2O$ in ethanol led to formation of mono-cationic [CuBr(N_2S_2)]Br complex in good yield. Occurrence of reaction was

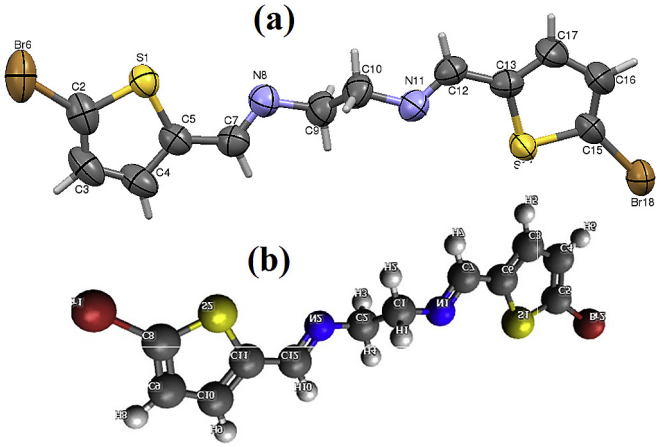

Fig. 2. (a) ORTEP of N_2S_2 free ligand with thermal ellipsoids drawn at 50% probability level, (b) optimized DFT-B3LYP structure.

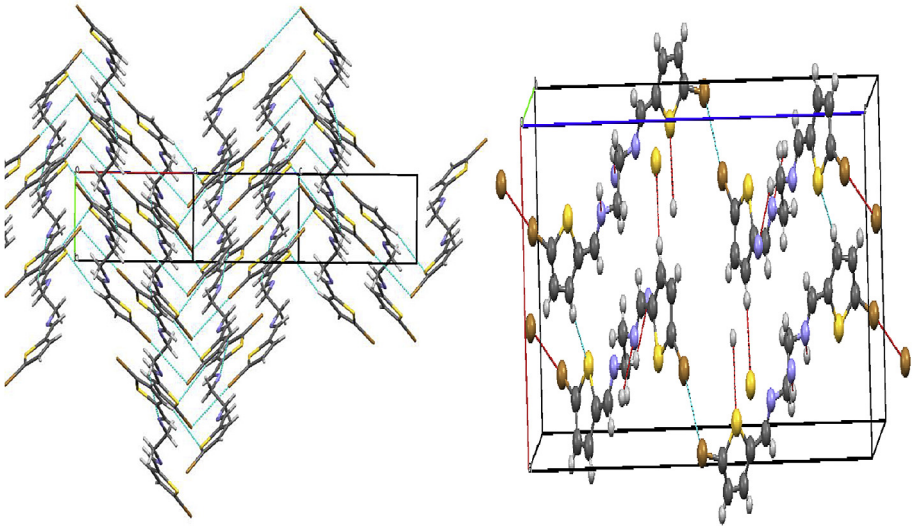

Fig. 3. The packing of molecules when viewed down the *a*-axis. The blue dotted lines indicate hydrogen bonds. (For interpretation of the references to colour in this figure legend, the reader is referred to the web version of this article.)

easily detected by the color change from brown to green upon mixing of the two reagents. The complex is soluble in water and other polar solvents such as DMF and is slightly soluble in alcohols.

Structures of the ligand and its complex were confirmed with the aid of MS, FT-IR, CV, NMR, UV–vis, EDS and TG/DTG, and with elemental analysis. The NMR spectra of the ligand were in total agreement with the assigned structure. Similarly, mass spectra for both the ligand and its complex displayed the molecular ions corresponding to the respective molecular formulas of prepared compounds.

Table 2
Bond angles (°) and bond lengths (Å) in the ligand.

Atoms	Length	Atoms	Length
S1-C2	1.717 (7)	C10-N11	1.454 (8)
S1-C5	1.724 (7)	N11-C12	1.261 (8)
C2-C3	1.360 (12)	C12-C13	1.446 (9)
C2-Br6	1.872 (8)	C13-C17	1.349 (9)
C3-C4	1.389 (12)	C13-S14	1.721 (6)
C4-C5	1.361 (9)	S14-C15	1.714 (6)
C5-C7	1.437 (9)	C15-C16	1.335 (10)
C7-N8	1.257 (8)	C15-Br18	1.870 (7)
N8-C9	1.459 (8)	C16-C17	1.406 (11)
C9-C10	1.501 (10)		
Atoms	**Angle**	**Atoms**	**Angle**
C2-S1-C5	91.1 (4)	N11-C10-C9	109.6 (5)
C3-C2-S1	112.0 (6)	C12-N11-C10	120.0 (6)
C3-C2-Br6	128.6 (6)	N11-C12-C13	121.4 (6)
S1-C2-Br6	119.5 (5)	C17-C13-C12	129.8 (6)
C2-C3-C4	112.3 (6)	C17-C13-S14	110.5 (6)
C5-C4-C3	113.8 (7)	C12-C13-S14	119.7 (5)
C4-C5-C7	127.8 (7)	C15-S14-C13	91.1 (3)
C4-C5-S1	110.8 (6)	C16-C15-S14	112.5 (5)
C7-C5-S1	121.4 (5)	C16-C15-Br18	127.7 (5)
N8-C7-C5	123.8 (6)	S14-C15-Br18	119.8 (3)
C7-N8-C9	116.9 (6)	C15-C16-C17	112.0 (6)
N8-C9-C10	112.4 (5)	C13-C17-C16	113.9 (6)

3.2. FT-IR and DFT-IR spectral analysis

FT-IR spectroscopy served to monitor the condensation reaction during N_2S_2 ligand formation. IR spectra of 5-bromothiophene-2-carbaldehyde and ethylenediamine were recorded before and after condonation as displayed in Fig. 1. Formation of the desired ligand was supported by two major changes: stretching vibration of C=O in the carbaldehyde at 1658 cm^{-1} (see Fig. 1a) was reduced by ~30 cm^{-1}, due to the C=N- (1629 cm^{-1}) ligand group formation, as in Fig. 1c and the primary N-H stretching vibrations in ethylenediamine at 3357 and 3281 cm^{-1} (see Fig. 1b) totally disappeared as shown in Fig. 1c.

DFT-IR theoretical calculations were also carried out for the N_2S_2 free ligand, as seen in Fig. 1d. The theoretical and experimental FT-IR spectra revealed an acceptable agreement. There was a small discrepancy, however, because the DFT-combinatorial calculations were performed for a free molecule in the gaseous state, whereas experimental results were obtained in the solid state, and are expected to be smaller than DFT-theoretical calculations [38,39]. On the other hand, the IR spectra of the synthesized [CuBr(N_2S_2)]Br complex showed similar IR-behavior to the N_2S_2 free ligand with slightly low chemical shifts, as displayed in Fig. 1e. In the complex,

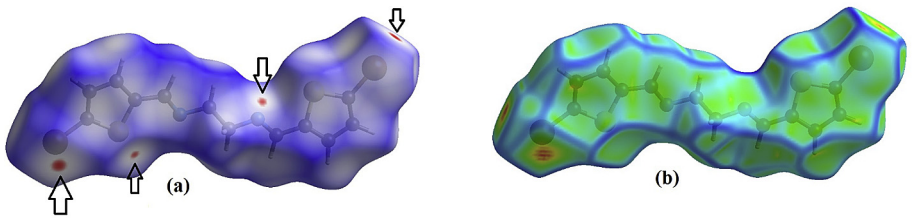

Fig. 4. d_{norm} mapped a) and curvedness b) on Hirshfeld surface for visualizing the inter-contacts of N_2S_2 ligand. Color-scale ranges between 0.18 au (blue) and 1.4 au (red). (For interpretation of the references to colour in this figure legend, the reader is referred to the web version of this article.)

water broad peaks vibrations at ~3380 $\nu_{(O-H)}$/1458 $\nu_{(bend)}$ are observed indicating the presence of uncoordinated water molecule. The $\nu_{(N=C)}$ band at 1608 cm^{-1} in the complex was shifted to a lower wavenumber (~21 cm^{-1}) compared to the ligand at 1629 cm^{-1}. Such result supports the formation of C=N→Cu(II) coordination bonds. The most important IR band, is the presence of a sharp peak at ~500 cm^{-1} (only in the complex spectrum) due to $\nu_{(Cu-N)}$ vibrations [22,40], which indicates the direct N→Cu(II) new bonds formation.

3.3. Crystal and optimized structure of N_2S_2

The molecular and optimized DFT-B3LYP structures of the ligand, along with atoms numbered, are depicted in Fig. 2, whereas Fig. 3 shows the packing of the ligand. In addition, bond lengths and bond angles of the non-hydrogen atoms are given in Table 2. The structures of the ligand revealed the anti-EE conformation around the C-C bond isomer in both C=N groups, as kinetics favored the isomer with less internal strict repulsion effect. This forces the S-heterocyclic rings and the C=N groups to be in the same plane but opposite in their directions making the structure suitable for two metal ions coordination as can be seen in Scheme 1.

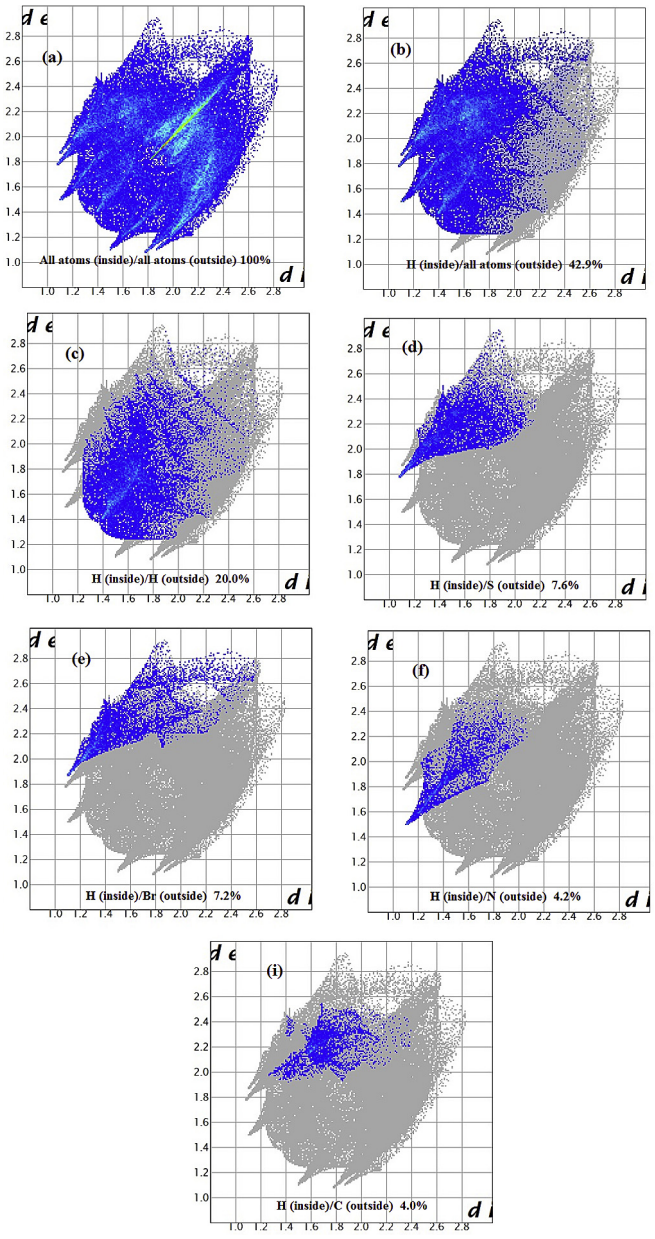

Fig. 5. Fingerprint of N_2S_2 ligand inside … outside atoms, (a) all … all, (b) H … all, (c) H…H, (d) H…S, (e) H…Br, (f) H…N and (i) H…C.

3.4. Hirshfeld surface analysis for N_2S_2 ligand

The Hirshfeld surface of N_2S_2 ligand is – shown in Fig. 4. The red spots over the surface reveal the inter-contacts involved in hydrogen bond bonds [41–45]. The dark-red spots on d_{norm} surface appear as a result of the short interatomic, i.e., strong H-bonds, while the other weak intermolecular interactions are in light-red spots.

The 2D Finger print plots over the Hirshfeld surfaces show the presence of inter-contacts H…H > H…S > H…Br > H…N > H…C. The major contribution is from an H…H, whereas the least contribution is from H…C as depicted in Fig. 5.

3.5. EDS investigations

The compositions of N_2S_2 ligand and its complex were determined by EDS analysis, as shown in Fig. 6. The change in the EDS of the ligand before and after coordination with Cu(II) supported the L→M complexation formed and allowed to differentiate their chemical compositions. Data from Fig. 6a showed that the ligand contains only C, N, S, and Br, whereas the complex contains C, N, S, Br, and Cu atoms as shown in Fig. 6b, which confirms complexation. On the other hand, the absence of uncited peaks reflected the purity of both the ligand and its complex. Absence of oxygen atom signs in the ligand or the complex indicate the stability of such compounds against atmospheric O_2 pressure.

3.6. ^1H and ^{13}C NMR investigation of the ligand

Experimental ^1H NMR analysis of N_2S_2 ligand was performed in $CDCl_3$ and the spectrum is illustrated in Fig. 7a. A typical ^1H NMR spectrum showed a sharp broad signal at δ 3.86 ppm due

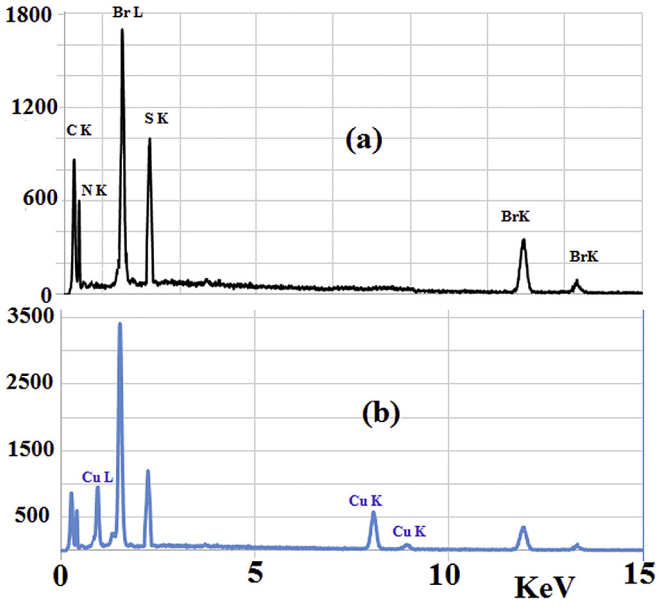

Fig. 6. EDS spectra of N_2S_2 ligand (a) and $[CuBr(N_2S_2)]Br$ complex (b).

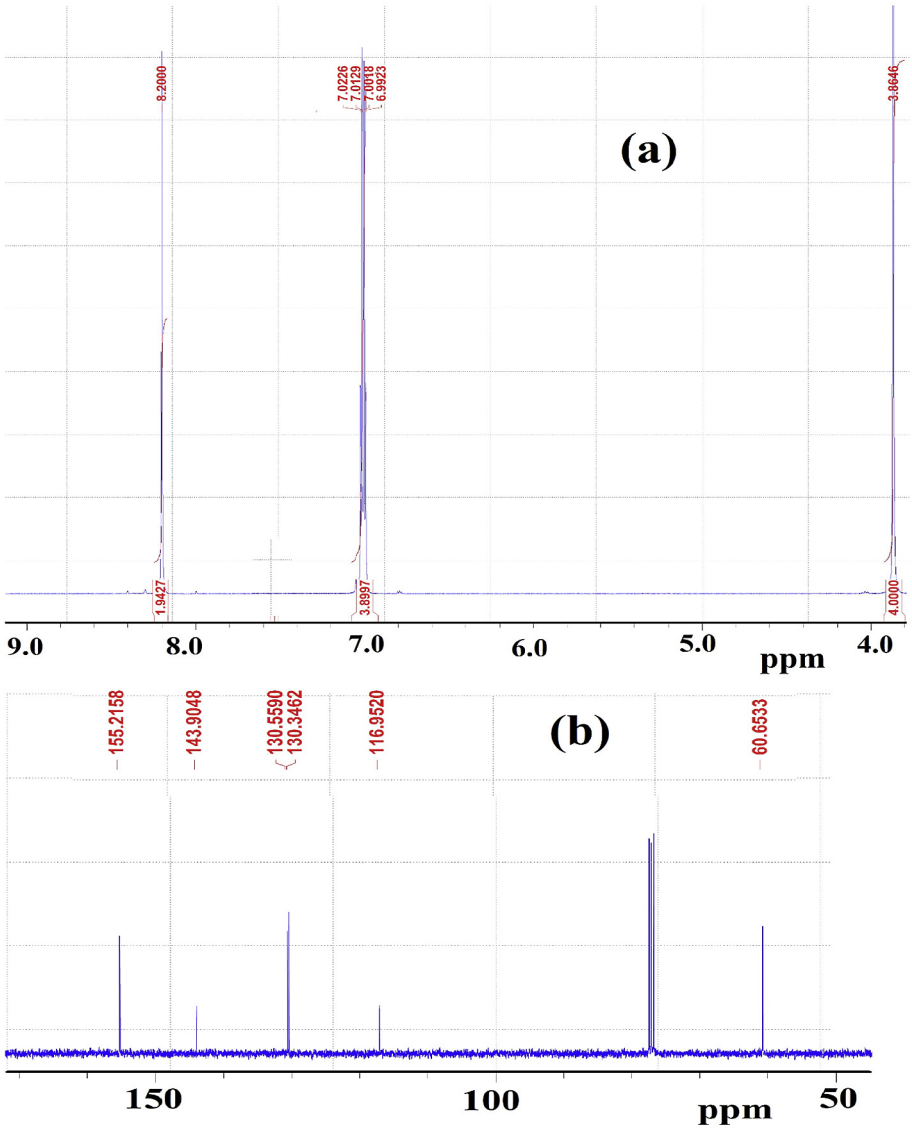

Fig. 7. NMR spectra of N_2S_2 ligand dissolved in $CDCl_3$ at RT (a) ^1H NMR and (b) ^{13}C NMR.

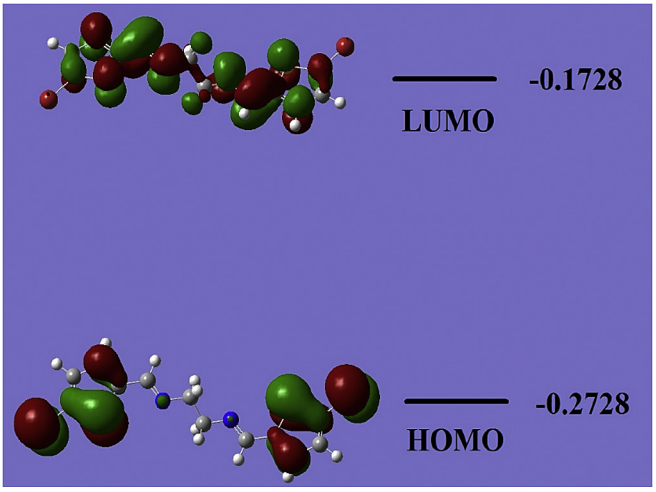

Fig. 8. HOMO/LUMO molecular orbitals plots of N_2S_2 ligand.

to $=NCH_2CH_2N=$. The thiophene protons resonated as two doublets at δ 6.99 and 7.01 ppm, with average $^3J_{AB}$ ~4.80 HZ, whereas the azomethine proton N=CH appeared as a singlet at 8.20 ppm.

The ^{13}C NMR spectrum of the ligand is shown in Fig. 7b. ^{13}C NMR spectrum revealed a signal at δ 60.6 ppm ($CH_2N=$), in addition to the four thiophene aromatic carbons resonated as singlets at δ 116.9, 130.3, 130.5, and 143.9 ppm. The signal observed at 155.2 ppm was attributed to the N=CH carbon.

3.7. Ligand frontier molecular orbital calculation

Calculation of the HOMO/LUMO energy levels are very helpful to predict the chemical behavior of the desired compounds. Several chemical parameters such as hardness, electrophilicity, symmetry, quantum chemistry terms, chemical potential, electronegativity, and local reactivity can be evaluated from the HOMO/LUMO energy gap [38,39]. Fig. 8 pictorially represents the HOMO/LUMO orbital shapes in the gaseous phase, the HOMO response at −0.2728 eV while the LUMO is located at −0.1728 eV with 0.100 eV energy gap. The value of the calculated energy gap indicates the easiness of HOMO to LUMO electron excitation, which shows that HOMOs are

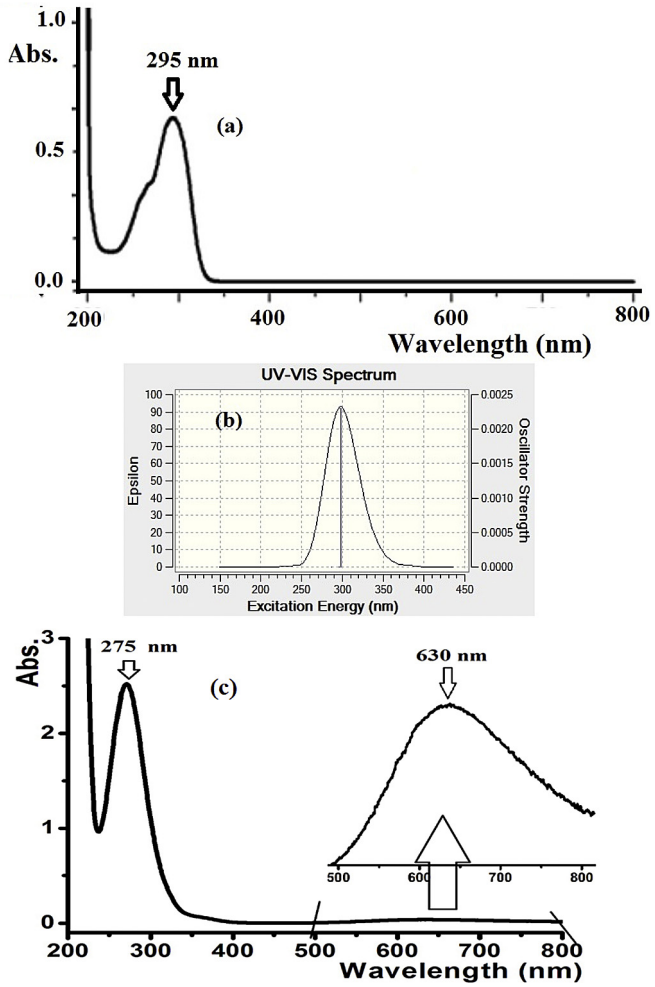

Fig. 9. UV–Vis. Spectroscopy spectra of 1×10^{-5} M of N_2S_2 ligand (a) experimentally in ethanol at RT, (b) TD-DFT/B3LYP/6–311++ (d,p) theoretically (in gaseous state) and (c) 1×10^{-5} M of [CuBr(N_2S_2)]Br complex dissolved in water at RT.

the dominant molecular orbitals which is consistent with the overall nature of the pentadentate ligand as a strong electron-donor with high degree of nuclophilicity. In addition, results reveal that it is very easy to excite electrons from ground to excited state with such small energy gap. HOMO and LUMO gap is related to the chemical reactivity or kinetic stability, since they both have negative values, which decides the chemical stability of the ligand [46].

3.8. UV–vis. TD-DFT/B3LYP/3–21 spectral

The electronic absorption behavior of N_2S_2 ligand and its complex are measured at room temperature. The absorption bands of the ligand are calculated by means of TD-DFT/B3LYP/6–311++(d,p) in gaseous state. The spectrum of the ligand (N_2S_2) demonstrated high intense transitions at λ_{max} = 295 nm (sharp) with ($\varepsilon = 6.5 \times 10^4$ $M^{-1}L^{-1}$) ascribed to π-π^* electron transition, as shown in Fig. 9a, the shoulder at 265 nm mostly attributed to n-π^*/σ^* electron transition. Furthermore, time-dependent DFT UV–vis spectrum absorption maximum was found at 297 nm (sharp) as displayed in Fig. 9b.

Results obtained from these Figures reveal an excellent agreement between the theoretical-TD-DFT and experimental UV-measurement was observed; the slight ~2 nm shift may be due to solvent effect [47–49]. In water, the complex [CuBr(N_2S_2)]Br revealed two signals; a sharp one in the UV region at $\lambda_{max} = 275$ nm ($\varepsilon = 1.2 \times 10^4$ $M^{-1}L^{-1}$) attributed to ligand π-π^* electron transition shifted down from 295 nm in the free N_2S_2 ligand due to the N_2S_2 →Cu(II) coordination, and a second broad band in the visible region at λ_{max} = 630 nm ($\varepsilon = 6.4 \times 10^2$ $M^{-1}L^{-1}$) due to DMSO-d_6 electron transition that belongs to the square pyramid geometry around Cu(II) centers [22] as seen in Fig. 9d.

3.9. Thermal analysis investigation

Thermal analyses (TG/DTG) were performed to obtain information about the stability of the ligand and its copper complex. This was achieved increasing the temperature from 0 to 1000 °C at a rate of 10 °C/min and under an open atmosphere. Displayed in Fig. 10a and b are TG/DTG curves for the ligand N_2S_2 and its complex, respectively. For the ligand, TG curve (Fig. 10a) revealed that there is a 100% mass loss over the temperature range of 60–110 °C. The ligand may simply sublimed or decomposed to light elements such as SO_2, NO_2, and CO_2, in a broad step (with ~100% Wt. lost) since no residue or intermediate degradation steps were observed. Therefore, the ligand undergoes a simple one-step thermal decomposition.

On the other hand, TG/DTG curve of the complex [CuBr(N_2S_2)]Br undergoes three main decomposition steps as depicted in Fig. 10b. Results revealed a mass loss of 2.7% in the range 60–80 °C attributed to loss of uncoordinated H_2O molecule; this agrees with IR results. In the temperature range of 260–370 °C, the complex loses N_2S_2 from the backbone of the complex to give pure $CuBr_2$ as indicated by a mass loss of 63%. In the temperature range of 580–680 °C, the complex loses 21.3% of its mass which is due to the oxide/bromide replacement reaction on $CuBr_2$ which eventually leads to production of copper oxide (CuO) with 14% of the mass.

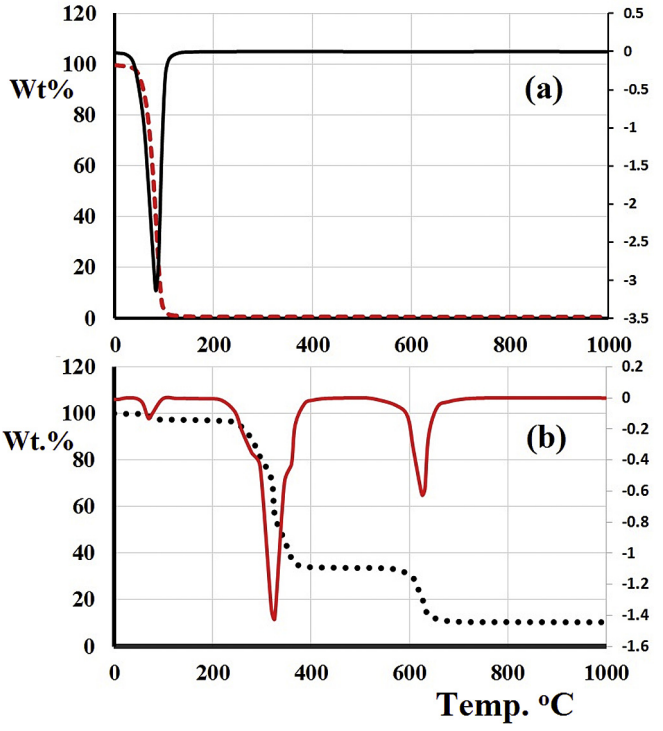

Fig. 10. TG/DTG thermal curves of: (a) the ligand and (b) [CuBr(N_2S_2)]Br complex.

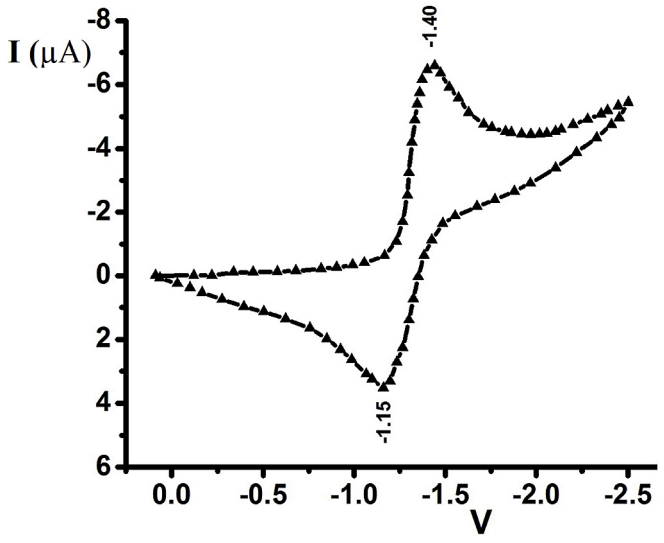

Fig. 11. Cyclic voltammogram recorded at 100 mV/s for reduction of a 0.10 mM of the complex [CuBr(N_2S_2)]Br at a platinum electrode in DMF containing 0.1 M TBAP.

3.10. Electrochemical behavior of the complex

Cyclic voltammetry was employed to investigate the electrochemical behavior of the [CuBr(N_2S_2)]Br complex. Potential was scanned from 0.1 to −2.6 V versus Ag/AgCl. Depicted in Fig. 11 is a cyclic voltammogram recorded at a scan rate of 100 mV/s for reduction of a 0.1 mM solution of the complex [CuBr(N_2S_2)]Br at a freshly polished platinum electrode in DMF containing 0.1 M TBAP. The voltammogram shows the reversible copper (II)–copper(I) redox couple with a cathodic peak potential (Epc) of −1.40 V and an anodic peak potential (Epa) of −1.15 V; ΔEp = 250 mV (ΔEp = Epa − Epc). Furthermore, the ratio Ipa/Ipc is close to unity. The reversible couple corresponds to a one electron-transfer as given in the following equation:

$$\left[Cu^{II}Br(N_2S_2)\right]Br \rightleftharpoons \left[Cu^{I}Br(N_2S_2)\right]$$

4. Conclusions

A new Schiff base ligand, (N^1E, N^2E)-N^1,N^2-bis((5-bromothiophen-2-yl)methylene)ethane-1,2-diamine (N_2S_2) was synthesized by condensation of 5-bromothiophene-2-carbaldehyde with ethylenediamine. The ligand has been characterized by means of various spectroscopic methods and its structure was confirmed by X-ray single crystal analysis as EE isomer for the first time. DFT/B3LYP theoretical calculations for N_2S_2 ligand are in total agreement with the experimental results. Additionally, the water soluble square pyramid mono-cationic [CuBr(N_2S_2)]Br was prepared and as square pyramid geometry around Cu(II) centers. TG result showed the N_2S_2 free ligand and its complex are decomposed by totally different mechanisms. The copper (II) complex, [CuBr(N_2S_2)]Br, exhibits reversible one-electron reduction to the corresponding copper(I) specie.

Acknowledgements

The authors extend their sincere appreciation to the Deanship of Scientific Research at king Saud University for its funding this Prolific Research group (PRG-1437-29).

Appendix A. Supplementary materials

"Crystallographic data for the structural analyses have been deposited with the Cambridge crystallographic data center, CCDC No. 1026142. These data can be obtained free of charge via www.ccdc.cam.ac.uk/conts/retrieving.html (or from the CCDC, 12 union Road, Cambridge CB2 IEZ, UK; fax: +44-1223-33633; e-mail: deposit@ccdc.ca.ac.uk)".

References

[1] M.L. Petrus, R.K.M. Bouwer, U. Lafont, S. Athanasopoulos, N.C. Greenham, T.J. Dingemans, J. Mater. Chem. A 2 (2014) 9474.
[2] T.P. Yoon, E.N. Jacobsen, Science 299 (2003) 1691.
[3] R. Nair, A. Shah, S. Baluja, S. Chanda, J. Serbian Chem. Soc. 71 (2006) 733.
[4] S. Ilhan, H. Baykara, M.S. Seyitoglu, A. Levent, S. Ozdemir, A. Dundar, A. Oztomsuk, M.H. Cornejo, J. Mol. Struct. 1075 (2014) 32.
[5] M. Gaber, N. El-Wakiel, H. El-Ghamry, S.K. Fathalla, J. Mol. Struct. 1076 (2014) 251.
[6] G. Grivani, G. Bruno, H.A. Rudbari, A.D. Khalaji, P. Pourteimouri, Inorg. Chem. Commun. 18 (2012) 15.
[7] S. Banerjee, C. Adhikary, C. Rizzoli, R. Pal, Inorg. Chim. Acta 409 (2014) 202.
[8] G. Grivani, A. Ghavami, M. Kučerakova, M. Dušek, A.D. Khalaji, J. Mol. Struct. 1076 (2014) 326.
[9] T. Wei, G. Gao, W. Qu, B. Shi, Q. Lin, H. Yao, Y. Zhang, Sens. Actuators B Chem. 199 (2014) 142.
[10] P. Fita, E. Luzina, T. Dziembowska, C. Radzewicz, A. Grabowska, J. Chem. Phys. 125 (2006) 4508.
[11] S. Amer, N. El-Wakiel, H. El-Ghamry, J. Mol. Struct. 1049 (2013) 326.
[12] K.S. Kumar, S. Ganguly, R. Veerasamy, E. De Clercq, Eur. J. Med. Chem. 45 (2010) 5474.
[13] O. Gungor, P. Gurkan, J. Mol. Struct. 1074 (2014) 62.
[14] P.A. Vigato, S. Tamburini, Coord. Chem. Rev. 248 (2004) 1717.
[15] S.M. Bensaber, H.A. Allafe, N.B. Ermeli, S.B. Mohamed, A. Zetrini, S.G. Alsabri, M. Erhuma, A. Hermann, M.I. Jaeda, A.M. Gbaj, Med. Chem. 23 (2014) 5120.
[16] A.K. Singh, S.K. Pandey, O.P. Pandey, S.K. Sengupta, J. Mol. Struct. 1074 (2014) 376.
[17] C.M. da Silva, D. da Silva, L.V. Modolo, R.B. Alves, M.A. de Resende, C.V.B. Martins, A. de Fatima, J. Adv. Res. 2 (2011) 1.
[18] M.L. Low, G. Paulus, P. Dorlet, R. Guillot, R. Rosli, N. Delsuc, K.A. Crouse, C. Policar, Biometals 28 (2015) 553.
[19] P.J. Holland, S.R. Barnard, H.M. Bayly, G.C. Betts, J.R. Churchill, R. Edge Dilworth, J.C. Green, R. Hueting, Eur. J. Inorg. Chem. 2008 (2008) 1985.
[20] M. Gennari, J. Pecaut, M.N. Collomb, C. Duboc, Dalton Trans. 41 (2012) 3130.
[21] I. Warad, O. Abd-Elkaderm, A. Boshaala, N. Al-Zaqri, B. Hammouti, T. Ben Hadda, Res. Chem. Intermed. 39 (2013) 721.
[22] M. Al-Noaimi, M. Choudhar, F. Awwadi, W. Talib, T. Ben Hadda, S. Yousuf, A. Sawafta, I. Warad, Spectrochim. Acta Part A. 127 (2015) 225.
[23] I. Warad, M. Al-Noaimi, M. Suleiman, W. Darwish, A. Bakheit, M. Abdoh, I. Saadeddin, N. Shivalingegowda, N. Lokanath, O. Bsharat, A. Barakat, Bioinorg. Chem. Appl. (2014) 1.
[24] P. Inamdar, R. Chauhan, J. Abraham, A. Sheela, Inorg. Chem. Comm. 67 (2016) 67.
[25] Z. Shokohi-pour, H. Chiniforoshan, A. Abbas, M. Borojeni, B. Notash, J. Photochem Photobiol. B Biol. 162 (2016) 34.
[26] R. Pradhan, M. Banik, D. Cordes, A. Slawin, N. Sah, Inorg. Chim. Acta 442 (2016) 70.
[27] L. Abdel-Rahman, A. Abu-Dief, M. Ismael, M. Mohamed, N. Hashem, J. Mol. Struc 1103 (2016) 232.
[28] L. Jia, J. Xu, X. Zhao, Sh Shen, T. Zhou, Zh Xu, T. Zhu, R. Chen, T. Ma, J. Xie, K. Dong, J. Huang, J. Inorg. Biochem. 159 (2016) 107.
[29] D. Palanimuthu, S.V. Shinde, K. Somasundaram, A.G. Samuelson, J. Med. Chem. 56 (2013) 722.
[30] C. Santini, M. Pellei, V. Gandin, M. Porchia, F. Tisato, C. Marzano, Chem. Rev. 114 (2014) 815.
[31] Bruker, APEX2, SAINT and SADABS, Bruker AXS Inc, Madison, Wisconsin, USA, 2009.
[32] G.M. Sheldrick, Acta Cryst. A 64 (2008) 112.
[33] A.L. Spek, Acta Cryst. A 46 (1990) 34.
[34] A.D. Becke, J. Chem. Phys. 98 (1993) 5648.
[35] M.J. Frisch, GAUSSIAN 09, Revision B.09, GAUSSIAN, Inc., Pittsburgh, PA, 2009.
[36] R. Krishnan, M.J. Frisch, J.A. Pople, J. Chem. Phys. 72 (1980) 4244.
[37] S.K. Wolff, D.J. Grimwood, J.J. McKinnon, D. Jayatilaka, M.A. Spackman, Crystal explorer 2.1, University of Western Australia, Perth, 2007.
[38] K. Fukui, Science 218 (1982) 747.
[39] J. Aihara, J. Phys. Chem. A 103 (1999) 7487.
[40] K. Nakamoto, Infrared and Raman Spectra of Inorganic and Coordination Compounds, fourth ed., J. Wiley & Sons, NY, 1986.
[41] A. Barakat, S.M. Soliman, H.A. Ghabbour, M. Ali, A.M. Al-Majid, A. Zarrouk, I. Warad, J. Molec. Struct. 1137 (2017) 354.
[42] M.A. Spackman, D. Jayatilaka, Cryst. Engg. Comm. 11 (2009) 19.

[43] M.A. Spackman, J.J. McKinnon, Cryst. Engg. Comm. 4 (2002) 378.
[44] R. Patela, N. Singha, K. Shuklaa, J. Niclos-Gutíerrezb, S. Astineirasb, V. Vaidyanathanc, B. Unni Nairc, Spectrochim. Acta Part A. 62 (2005) 261.
[45] I. Warad, F. Al-Rimawi, A. Barakat, S. Affouneh, N. Shivalingegowda, N.K. Lokanath, I.M. Abu-Reidah, Chem. Cen. J. 10 (2016) 38.
[46] I. Warad, A. Barakat, J. Molec. Strut 1134 (2017) 17.
[47] S. Sebastian, S. Sylvestre, J. Jayabharathi, S. Ayyapan, M. Amalanathan, K. Oudayakumar, I. Herma, Spectrochim. Acta Part A 136 (2015) 1107.
[48] S. Tarchouna, I. Chaabane, A. Ben Rahaiem, Phys. E. 83 (2016) 186.
[49] H. Golchoubian, E. Rezaee, Polyhedron 55 (2013) 162.